Millimeter-Wave Permittivity of a 93-mm-Diameter Single-Crystal AlN Wafer

Chunyi Li[1], Xinghao Tong[1], Tianze Li[1], Lei Li[1], James C. M. Hwang[1], Kasey Hogan[2], James Grandusky[2], Shana Yanagimoto[3], Yoshiyuki Yanagimoto[3]

[1]Cornell University, Ithaca, NY, USA, [2]Crystal IS Inc., Green Island, NY, USA, [3]EM labs Inc., Kobe, Japan

Abstract — **Single-crystal bulk AlN is an emerging material for high-power and high-frequency applications due to its ultrawide bandgap, high thermal conductivity, and compatibility with GaN-based heterostructures. However, permittivity data for single-crystal bulk AlN at millimeter-wave frequencies remain scarce, mainly due to challenges for sizable wafers and high-frequency measurements. Recently, we have overcome these challenges to characterize the permittivity of 2”-diameter AlN wafers at microwave and millimeter-wave frequencies. For scaling from 2” to 100 mm, we report in this work the permittivity of a 93-mm diameter wafer measured from 54 to 320 GHz. Within this frequency range, the dielectric constant is found to be constant at 7.80 ± 0.01, while the loss tangent increases linearly with frequency according to $(1.1 \pm 0.1)\cdot 10^{-4}\cdot[1 + (1.5 \pm 0.3)\cdot 10^{-11}f]$, where f is frequency in Hz. These results are consistent with that of 2” wafers, indicating potential for scaling to 100 mm for production at most compound-semiconductor foundries.**

Index Terms — **Aluminum nitride, dielectric constant, Fabry-Perot resonator, loss tangent, millimeter wave, permittivity**

I. INTRODUCTION

AlN has played a key role in electronics for decades, with polycrystal AlN valued for its high thermal conductivity in semiconductor packages and its high piezoelectric coefficient, acoustic velocity, and acoustic impedance in acoustic filters. With the recent availability of large single-crystal AlN wafers, attention has shifted towards their use in high-power, high-frequency transistors. Their ultra-wide bandgap, high thermal conductivity, and excellent mechanical properties make AlN an ideal native substrate for epitaxial growth of GaN high-electron mobility transistors (HEMTs), offering superior structural compatibility, reduced lattice mismatch, and lower thermal boundary resistance compared with GaN HEMTs on foreign substrates such as Si, SiC, or sapphire. These advances enable higher-power and higher-frequency performance, improved efficiency, and greater reliability.

As the development of single-crystal AlN wafers continues, 100-mm wafers have recently become available, addressing key challenges of size, cost, and production capacity for commercial device fabrication [1]. However, the wafer quality has not been fully evaluated, and parameters such as permittivity, critical for assessing material quality and enabling device design and modeling, have yet to be characterized.

Permittivity ε is a fundamental material property that governs the electromagnetic wave propagation and attenuation. It is a complex number given by

$$\varepsilon = \varepsilon_0 \varepsilon_R = \varepsilon_0\left(\varepsilon'_R - j\varepsilon''_R\right) = \varepsilon_0 \varepsilon'_R (1 - j\tan\delta), \qquad (1)$$

where ε_0 is the vacuum permittivity, ε_R is the relative permittivity, ε'_R is the real part of ε_R representing the material’s ability to store energy from an external field, and ε''_R is the imaginary part of ε_R associated with energy dissipation. The ratio $\tan\delta = \varepsilon''_R / \varepsilon'_R$ is commonly referred to as the loss tangent, while ε'_R is often called the dielectric constant. For low-loss materials, $\tan\delta << 1$, and $\varepsilon_R \approx \varepsilon'_R$.

To date, there are only three reports on permittivity of single-crystal bulk AlN [2]–[4], but they are either below 10 MHz or above 1 THz, leaving out microwave and millimeter-wave frequencies. Recently, we filled in this knowledge gap by characterizing the permittivity of multiple 2” AlN wafers of thickness ranging from 206 to 549 μm and found weak thickness and temperature dependence [5]. Additionally, across the measured frequencies 10–320 GHz, ε_R is constant and $\tan\delta$ linearly increases with frequency. Therefore, averaging across all frequencies and thicknesses,

$$\varepsilon_R = 7.805 \pm 0.007, \qquad (2)$$

and

$$\tan\delta = (0.78 \pm 0.01)\cdot 10^{-4} \cdot \left[1 + (2.22 \pm 0.02)\cdot 10^{-11} f\right], \qquad (3)$$

where f is frequency in Hz.

In this work, we have characterized the permittivity of a 93-mm wafer thinned to approximately 250 μm and found the result highly consistent with (2) and (3).

II. MEASUREMENT

A. Setup and Procedure

The measurement setup and procedure follow that of [5]. Fig. 1(a) shows the general setup in which a vector network analyzer (Anritsu MS4647B, 10 MHz to 70 GHz) is connected through a pair of frequency extenders (Virginia Diodes) to a Fabry-Perot resonator (EM labs) placed in between. To cover 54 to 320 GHz, three sets of frequency extenders and resonators are

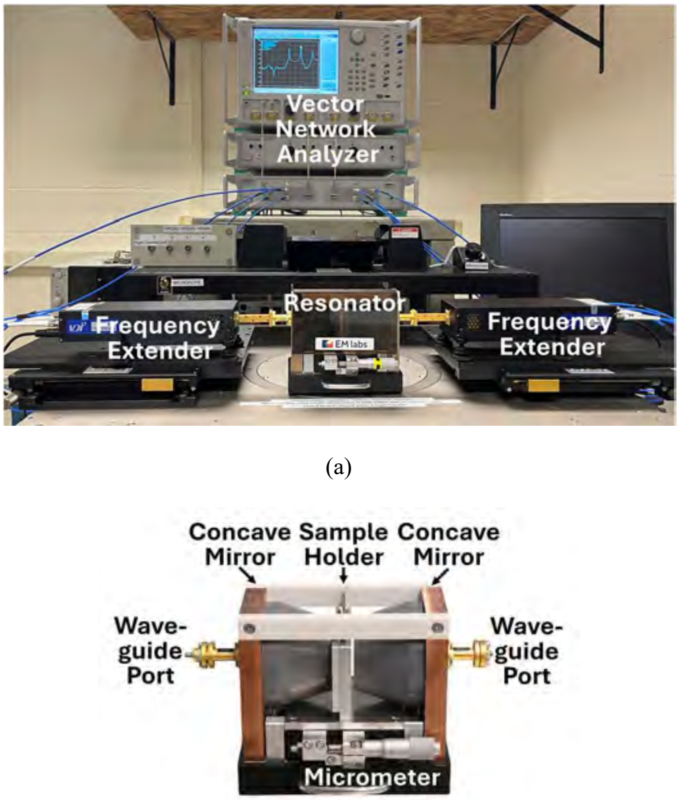

(a)

(b)

Fig. 1. (a) Permittivity measurement setup. (b) Resonator details.

used: broadband (25–110 GHz), D band (110–170 GHz), and J band (220–330 GHz).

Each Fabry-Perot resonator consists of two concave, confocal copper mirrors with a radius of curvature of $r = 96$ mm [Fig. 1(b)]. The high conductivity of copper ensures strong reflectivity. Because the resonator is based on an air cavity, its quality factor can reach the 10^5 range, allowing $\tan\delta$ measurement as low as 10^{-5}. Such high-Q resonators are critical for characterizing ultra-low-loss materials. Transverse electromagnetic waves are excited either by loop antennas (for the broadband resonator) or by waveguide ports (for D-band and J-band resonators) located at the centers of the mirrors. The sample holder is positioned in the middle of the resonator, and the wafer is clamped between two stainless steel plates to ensure that it remains flat and perpendicular to the mirrors.

For broadband measurements, the sample holder consists of a pair of 107 mm × 94 mm × 1 mm plates with center holes 63 mm in diameter. For D-band and J-band measurements, the holder consists of a pair of 63 mm × 55 mm × 1 mm plates with center holes approximately 25 mm in diameter. In general, the hole size should be an order of magnitude larger than the measurement wavelength to ensure most of the Gaussian-shaped beam, with a waist radius of approximately three wavelengths, passes through the hole. This why the hole size is bigger in the broadband resonator than in the D-band and J-band resonators.

With a mirror separation of $d = 120$ mm and the vacuum speed of light $c \approx 3 \times 10^{10}$ cm/s, resonances occur at

$$f_N = Nf_0 + (1/\pi)\arccos(d/r - 1), \tag{4}$$

where $N = 1, 2, 3 \ldots$ and $f_0 = c/2d \approx 1.25$ GHz. The wafer experiences the maximum electric field only at even N, where standing-wave antinodes are located in the middle of the resonator. To this end, the lateral position of the sample holder relative to the mirrors is fine-tuned with a micrometer to ensure the wafer is at an antinode.

Initially, the transmission coefficient S_{21} is measured across the resonator at different frequencies without the wafer to identify resonances at f_N, from which the quality factor is extracted as $Q_N = f_N/BW$, where BW is the 3-dB bandwidth of the resonance. The wafer is then clamped in the sample holder, inserted into the resonator, and its position fine-tuned with a micrometer. With the wafer in place, the resonances red-shift to f'_N and Q_N degrades to Q'_N. For low-loss materials, ε_R is only a function of the shift in f, while $\tan\delta$ is only a function of the degradation in Q. Therefore, the shift in f and degradation in Q can be used to extract ε_R and $\tan\delta$, respectively [6].

B. Samples

Single-crystal hexagonal wurtzite AlN boule is grown by physical vapor transport in a radio-frequency heated crucible [1]. The boule is oriented by x-ray diffraction to target a miscut of 0.2° off the (0001) plane to facilitate epitaxial growth, then sliced by a multi-wire saw with abrasive diamond slurry. After a wafer is sawed and edge-beveled, its top (Al) and bottom (N) faces are both ground to remove sawing-induced subsurface damage and to flatten the wafer. (The top and bottom faces are defined by the growth direction.) In turn, the grinding-induced damage is removed by chemical-mechanical polishing (CMP). The polishing rate of the Al face is much slower than the rate of the N face, leading to a so-called “epitaxy-ready” finish on the Al face and an optical finish on the N face. (Most epitaxial growers prefer to grow on the Al face, whereas the optically finished N face facilitates optical inspection and characterization.) After CMP, the wafer thickness of approximately 500 μm is halved. Mechanically, AlN is so strong that even with a thickness of approximately 250 μm, a free-standing wafer can be handled by standard semiconductor tools without any carrier.

Although the eventual target diameter is 100 mm, a 93-mm diameter wafer is first sacrificed for permittivity characterization before more wafers are produced at 100 mm. The whole wafer is used for broadband measurements to fit the 63-mm holes in the sample holder. After broadband measurements, the wafer is diced into four quarters to fit the D-band and J-band resonators and to cover most of the 25-mm holes of their sample holders. Using a spring-loaded mechanical stylus the thickness at the center of each quarter is measured as 235, 236, 243, and 247 μm, reflecting nonuniform CMP. All four quarters are measured at the D band, while one quarter is further measured at the J band. To ensure precision and repeatability, measurements are conducted in air under controlled temperature and humidity. Broadband measurements take place at 19 ± 1 °C and 38 ± 1% relative humidity, D-band measurements take place at 23 ± 1 °C and 22 ± 1% relative humidity, and J-band measurements take place at 21 ± 1 °C and 47 ± 1% relative humidity, reflecting seasonal changes. The effect of this level of temperature and humidity variations on the permittivity of AlN is expected to be negligible as on the permittivity of SiC [7].

III. RESULTS AND DISCUSSION

Fig. 2 shows the measured permittivities from 54 to 320 GHz. It can be seen that even after expanding ε_R to the second digit, there is no significant thickness or frequency dependence, except the linear frequency dependence of tanδ (coefficient of determination $R^2 > 0.93$). This confirms both the uniformity of the wafer and the reproducibility of the measurement.

Averaging across thicknesses and frequencies,

$$\varepsilon_R = 7.80 \pm 0.01, \tag{5}$$

and

$$\tan\delta = (1.1 \pm 0.1) \cdot 10^{-4} \cdot \left[1 + (1.5 \pm 0.3) \cdot 10^{-11} f\right] . \tag{6}$$

These results are very similar to (2) and (3), indicating comparable crystal quality between 2” and 93-mm AlN wafers, thinned or not.

Fig. 3 compares the D-band tanδ of this 93-mm AlN wafer, 2” AlN wafers, as well as other low-loss materials. It can be seen that although the 93-mm AlN wafer is a little lossier than 2” AlN wafers are, they are both comparable to fused silica, a common low-loss material. This indicates the high quality of larger AlN wafers making them suitable for volume production in most compound semiconductor foundries.

The AlN measured in this work is an anisotropic crystal sliced along the (0001) plane. With TEM waves at normal incidence, ordinary (in plane) permittivity is measured. To measure extraordinary (out of plane) permittivity, we can use a radial resonator [8] or a substrate-integrated waveguide [9] as has been demonstrated in SiC. Following the same approaches, we plan to measure the extraordinary permittivity of single-crystal AlN. This is important because electromagnetic waves propagating in microstrip and coplanar transmission lines fabricated on AlN are governed by both ordinary and extraordinary permittivities. The difference between ordinary and extraordinary permittivities can be as large as 25% [5], which is too large to be ignored.

IV. CONCLUSION

The millimeter-wave permittivity of a 93-mm diameter single-crystal AlN wafer is measured from 54 to 320 GHz using high-quality Fabry–Perot resonators. The measured ε_R is constant at 7.80 ± 0.01, with no significant thickness or frequency dependence, while the tanδ linearly increases with frequency from $1.5 \cdot 10^{-4}$ to $5.8 \cdot 10^{-4}$ and can be fitted with $(1.1 \pm 0.1) \cdot 10^{-4} \cdot [1 + (1.5 \pm 0.3) \cdot 10^{-11} f]$. This loss is comparable to that of fused silica, a common low-loss material, which confirms the high quality and uniformity of the AlN wafer, the reproducibility of the measurement, and the potential of large-diameter AlN wafers for production of high-frequency, high-power devices.

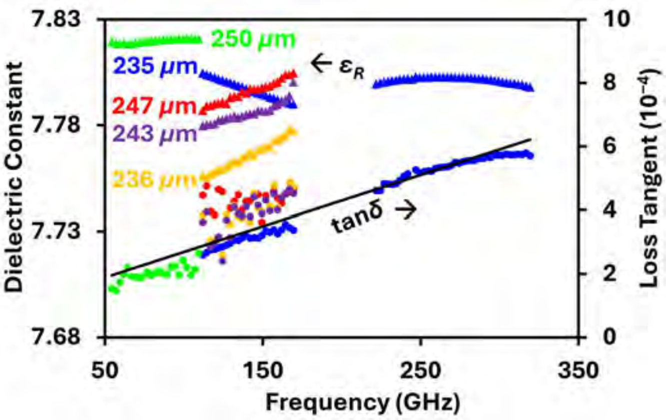

Fig. 2. Dielectric constant ε_R and loss tangent tanδ measured on a 93-mm diameter single-crystal AlN wafer. The whole wafer with a center thickness of 250 μm is measured from 54 to 110 GHz. Then it is diced into four quarters, with center thicknesses of 235, 236, 243, and 247 μm. All four quarters are then measured from 110 to 170 GHz, with the 235-μm quarter also measured from 220 to 320 GHz. It can be seen that, even after expanding ε_R to the second digit, there is no significant thickness or frequency dependence, except the linear frequency dependence of tanδ.

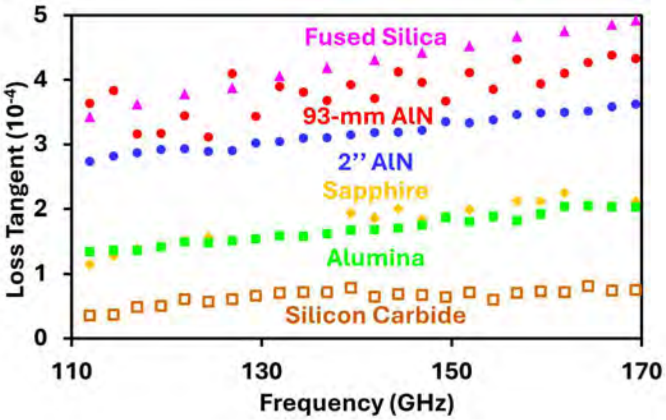

Fig. 3. D-band loss tangent of low-loss materials.

ACKNOWLEDGEMENT

We thank Dr. Jon Martens of Anritsu USA for his technical assistance. This work is supported in part by the U.S. National Science Foundation under Grants ECCS-2117305 and ECCS-2132323, in part by the U.S. Army Research Office under Grants W911NF2410023 and W911NF2510002, in part by the

U.S. Department of Defense through the NORDTECH Microelectronics Commons Hub under Contract Noo164-23-9-G061, and in part by SUPREME, one of the seven centers sponsored by the Semiconductor Research Corporation and the U.S. Defense Advanced Projects Agency through the Joint University Microelectronics Program 2.0 under Contract 2023-JU-3137.

REFERENCES

[1] R. T. Bondokov, K. Hogan, G. Q. Norbury, S. Matsumoto, and J. Grandusky, "Development of 100 mm AlN single-crystal growth and subsequent substrate preparation," *Phys. Status Solidi B,* p. 2500032, Mar. 2025.

[2] A. V. Sotnikov, H. Schmidt, E. P. Smirnova, T. Yu. Chemekova, and Y. N. Makarov, "Elastic and piezoelectric properties of AlN and $LiAlO_2$ single crystals," *IEEE Trans. Ultrason. Ferroelectr. Freq. Control,* vol. 57, no. 4, pp. 808–811, Apr. 2010.

[3] A. Majkić *et al.*, "Optical properties of aluminum nitride single crystals in the THz region," *Opt. Mater. Express*, vol. 5, no. 10, pp. 2106–2106, Sep. 2015.

[4] T. Kim, J. Kim, R. Dalmau, R. Schlesser, E. Preble, and X. Jiang, "High-temperature electromechanical characterization of AlN single crystals," *IEEE Trans. Ultrason. Ferroelectr. Freq. Control*, vol. 62, no. 10, pp. 1880–1887, Oct. 2015.

[5] Y. Yanagimoto, S. Yanagimoto, K. Hogan, J. Grandusky, C. Li, and J. C. M. Hwang, "Microwave and millimeter-wave permittivities of single-crystal AlN, including thickness and temperature dependence," *IEEE J. Microw.*, vol. 6, no. 1, pp. 1−9, Jan. 2026.

[6] A. L Cullen and P. K. Yu "The accurate measurement of permittivity by means of an open resonator," *Proc. R. Soc. London, Ser. A,* vol. 325, no. 1563, pp. 493–509, Dec. 1971.

[7] T. Li, L. Li, X. Wang, J. C. M. Hwang, S. Yanagimoto, and Y. Yanagimoto, "Ordinary and extraordinary permittivities of 4H SiC at different millimeter-wave frequencies, temperatures, and humidities," *IEEE J. Microw.*, vol. 4, no. 4, pp. 666–674, Sep. 2024.

[8] Y. Kato and T. Arakawa, "Broadband perpendicular permittivity measurements up to 220 GHz using a balanced-type circular disk resonator without air gap errors," *IEEE Trans. Instrum. Meas.,* vol. 74, p. 6007708, May 2025.

[9] L. Li, S. Reyes, M. Javad Asadi, P. Fay, and J. C. M. Hwang, "Extraordinary permittivity characterization of 4H SiC at millimeter- wave frequencies," *Appl. Phys. Lett.,* vol. 123, no. 1, p. 012105, Jul. 2023.